Polymer Bulletin 28, 717–723 (1992)

Polymer Bulletin

Assignment of acoustic emission to the failure sequence and damage zone growth in glass fiber strand mat-reinforced structural nylon RIM composites

J. Karger-Kocsis[1,*], Q. Yuan[1], and T. Czigány[2]

[1]Institut für Verbundwerkstoffe GmbH, Universität Kaiserslautern, Postfach 3049, W-6750 Kaiserslautern, Federal Republic of Germany
[2]Institute of Machine Parts Design, Technical University of Budapest, H-1111 Budapest, Hungary

ABSTRACT

The failure sequence and the damage zone evolution of a reaction injection molded (RIM) ≈20 wt.% glass strand mat reinforced nylon block copolymer (NBC) was studied by acoustic emission (AE) and transmitted light microscopy. Simultaneous monitoring of the failure mode by AE and transmitted light microscopy lead to a highly reliable discrimination between the observed failure and the related AE signal characteristics based on their amplitude and energy. The failure sequence consisted of the following steps: a) fiber debonding due to crack tip blunting, b) network-type deformation of the GF mat in the relative "soft" matrix with concomitant fiber debonding and voiding, c) bending of the strands with crack opening encouraged by matrix yielding, d) fracture of the bent strands and their filaments followed by pull-out processes. The evolution of the damage zone was also assessed by AE via localization and mapping of the related AE events. It was concluded that the damage zone reaches its maximum extension into the load direction (≈22 mm) at the maximum load. Further loading of the compact tension (CT) specimen decreases this size of the damage zone but strongly increses its extension perpendicular to it, i.e. along the crack growth direction.

1.INTRODUCTION

The target application fields (e.g.automotive, appliances) of polyamide structural (reinforcement present in continuous form, S) RIM composites make inevitable the characterization of the mechanical properties (e.g. fracture, fatigue, impact, stress corrosion cracking) and the related failure behavior about which limited informations are available by now [1-5]. Aims of the investigations reported here were to contribute to this topic by detecting the basic failure events and by assigning them to the related AE signal characteristics. A further intention of this study was to assess the damage zone and to follow its development during loading in (swirl) glass fiber (GF) strand mat reinforced nylon block copolymer (NBC) SRIM composites.

*Corresponding author

2.EXPERIMENTAL

2.1.Specimens

The molding and characteristics of the materials investigated were described in our previous works [1-5]. From the NBC-SRIM plates with ≈ 20 wt.% GF-mat content modified compact tension (CT) specimens were cut as depicted schematically in Figure 1.

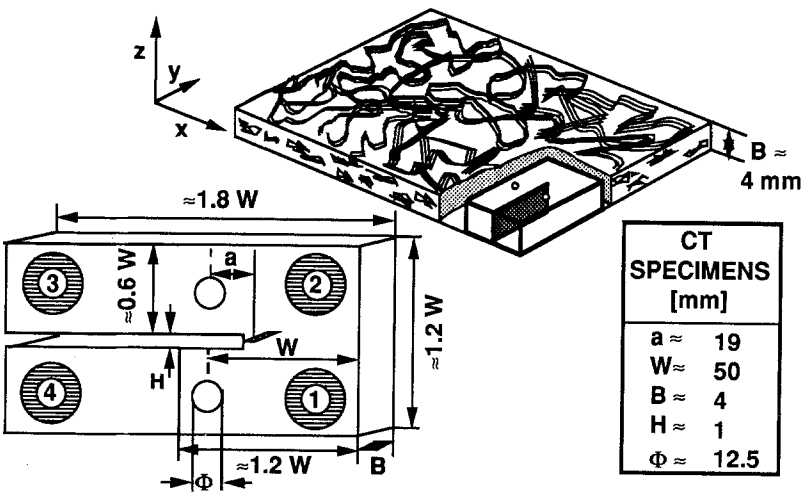

Figure 1 Structure of the GF mat reinforced SRIM composites schematically, and dimension of the enlarged CT-specimens used. This figure depicts also the positioning of the AE sensors in localization mode.

2.2.Tests

Loading of the enlarged CT-specimens (cf.Figure 1) was performed on a Zwick 1445 type tensile machine at ambient temperature and at v=1 mm/min crosshead speed. The failure behavior of the CT specimens was studied in-situ by a traveling light microscope. In order to distinguish among the different failure events evidenced by light microscopy, the acoustic emission (AE) of the specimen was also monitored during the loading.

AE was detected by a Defektophone NEZ 220 analyzer (Central Research Institute for Physics, Budapest, H) using wide bandwith transducers (20-1000 kHz) with built-in preamplifier. The signals were further amplified logarithmically. AE events were collected during the loading of the CT-specimen with a four sensor array (cf. Figure 1). This permitted the localization of the AE events based on the first hit principle in the knowledge of the acoustic wave propagation speed determined before (1300 m/s). During the tests the following primary AE signals were acquisited in floating mode: elapsed time, ringdown count, rise time, event duration,peak amplitude, events number, absolute average additionally to the external parameter (force) coming from the tensile machine. The PC software enabled different handling and displaying of the data.

3.RESULTS AND DISCUSSION

3.1.Failure sequence

Figure 2 displays the force - load line displacement (F-v_{LL}) curve of the CT-specimen together with the course of the cumulative AE events. The F-v_{LL} curve was "fragmented" (cf. I to V in Figure 2) in order to assure a confident assignment of the AE signals to the failure manner observed (cf. Figure 3). The series of the related bright field photographs taken during the loading of the CT-specimen are envisaged in Figure 3.

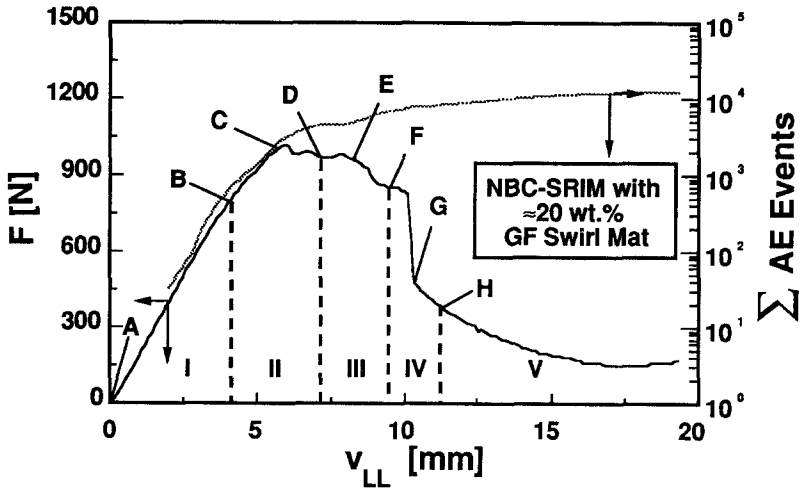

Figure 2 F-v_{LL} curve and the cumulative run of the AE events taken in localization mode for a modified CT-specimen. Note:this figure displays both the taking positions of the microphotographs in Figure 3 and the "fragmentation" of the curve for AE signal analysis.

Detailed examination of the measured and calculated AE parameters resulted that the observed failure mode can be best correlated with the AE signals when their amplitude and energy distribution in the chosen sections of the F-v_{LL} curve are considered. Thus Figure 4 informs about the differential distribution of the amplitude and energy of the AE events for each selected fraction of the loading curve (cf. Figure 2). Comparing the microscopically observed failure events at the crack tip (Figure 3) with those of the AE signal characteristics (Figure 4) for each section of the force-displacement curve the following assignments can be made [6]:

I Matrix deformation by crack tip blunting (amplitude ≈30 dB, energy≈10^{-7} pJ) which induces debonding and splitting-up of the strand right ahead of the crack tip (amplitude ≈ 60 dB, energy ≈ 10^{-3} pJ).

II Strands laying parallel and in the plane of the further crack growth debond in a longer range and split up (amplitude ≈ 50-75 dB, energy ≈ 10^{-6}...10^{-2} pJ) partially under fracture of their constituting filaments (amplitude ≈ 80-85 dB, energy ≈ 10^{-3}..10^{0} pJ). This debonding and fibrillation is a rather complicated process consisting of short and long

range debonding, splitting-up of the strand, fiber/matrix and fiber/fiber friction, therefore the AE signals can be found in a very broad range.

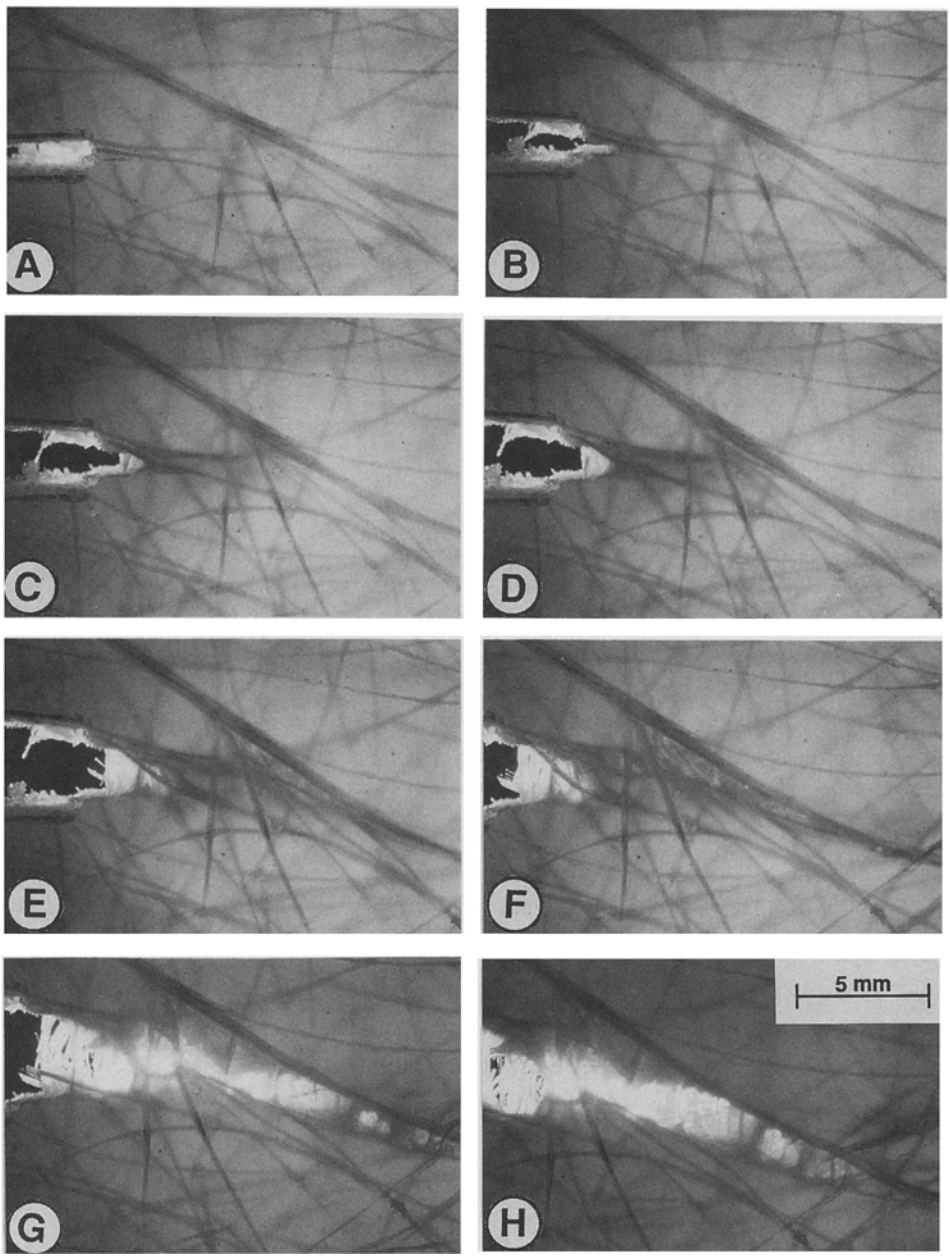

Figure 3 Serial bright field light microscopic pictures taken during the loading of the CT-specimen. Note: taking position of the pictures is marked in the related F-v_{LL} curve in Figure 2.

III Debonding (amplitude ≈ 40-45 dB, energy ≈ 10^{-6} pJ) and splitting-up (amplitude ≈ 60 dB, energy ≈ 10^{-3} pJ) of the strands dominate here. The former process takes place along the strands laying inclined with a small angle in respect to the expected crack growth plane.

IV In this stage of stable crack propagation the matrix fails by formation of voids, and void coalescence and thus by an enhanced tearing (amplitude ≈25 dB, energy: $10^{-9}..10^{-7}$ pJ). Among the fiber-related failure manners strand debonding (amplitude ≈ 60 dB, energy ≈ 10^{-4} pJ) and breakage of their constituting filament being under local bending stresses (amplitude ≈ 85 dB, energy ≈ 10^{-2} pJ) can be evidenced.

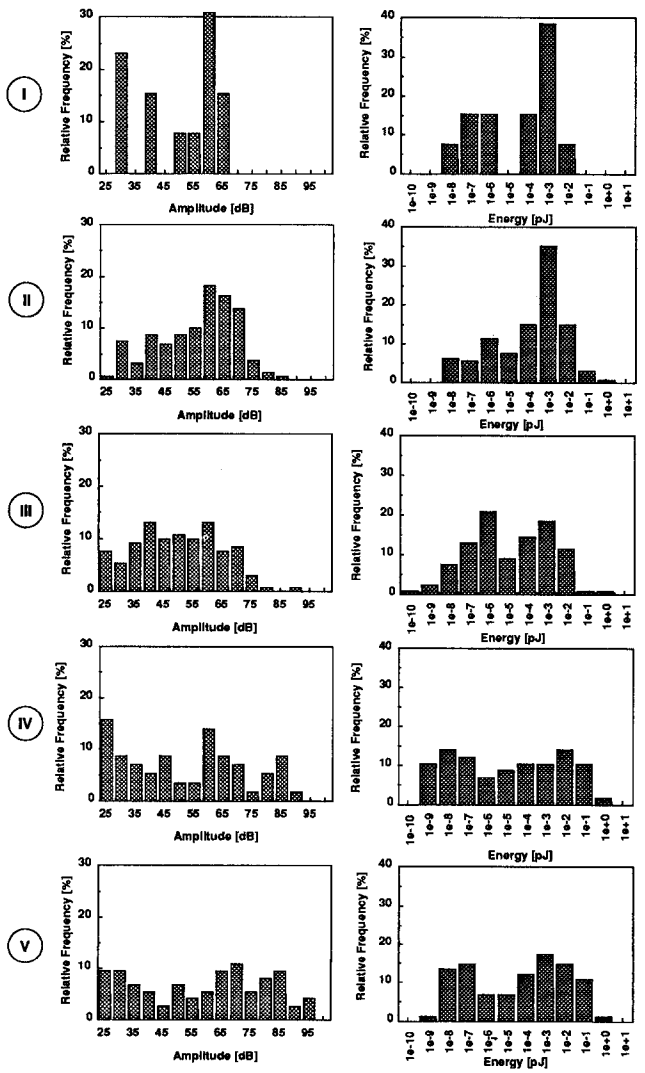

Figure 4 Relative amplitude and energy distribution of the AE events in different fragments of the F-v_{LL} curve in Figure 2. Notes: the corresponding light microscopic pictures are portrayed in Figure 3, whereas the run of the cumulative AE events in Figure 2.

V The relative amplitude distribution clearly indicates that in this final stage of fracture all previously mentioned failure events are involved (matrix deformation with an amplitude of ≈ 25 dB, short and long range debonding with 50 and 70 dB, respectively; filament fracture of bent strands at 95 dB). Since the further network deformability of the mat is locally hindered and thus the strands are fully extended into the loading direction; they fracture under tensile stresses generating AE signals of high amplitude (amplitude≈95 dB).

3.2.Size of the damage zone

The evolution of the damage zone concluded from the localized AE events can be followed by Figure 5. It is very interesting that the mapped AE events in the stages I and II indicate for a much larger damage area in localization mode than it could be concluded from the failure sites microscopically observed. The latter seems to occur only in the close vicinity of the crack tip. This effect is related with the local arrangement of the GF-mat and thus with the local load distribution. In the following stages (cf. III to V in Figures 2 to 4) the size of the damage zone, taken into the loading direction, decreases, whereas perpendicular to it, i.e. into the crack growth direction, the damage zone extends considerably. It can be concluded therefore, that the appearance of the load maximum is related with with the development of a critical damage zone size. This is probably a function of the mean mesh size and thus of the surface weight of the GF-mat. In our case this critical size can vell be estimated by a circle of ≈ 22 mm diameter, of which ≈ 15 mm strecthes into the free ligament. This value is very closely matched to the critical ligament width (≈12 mm) deduced recently from high-speed impact bending tests [5].

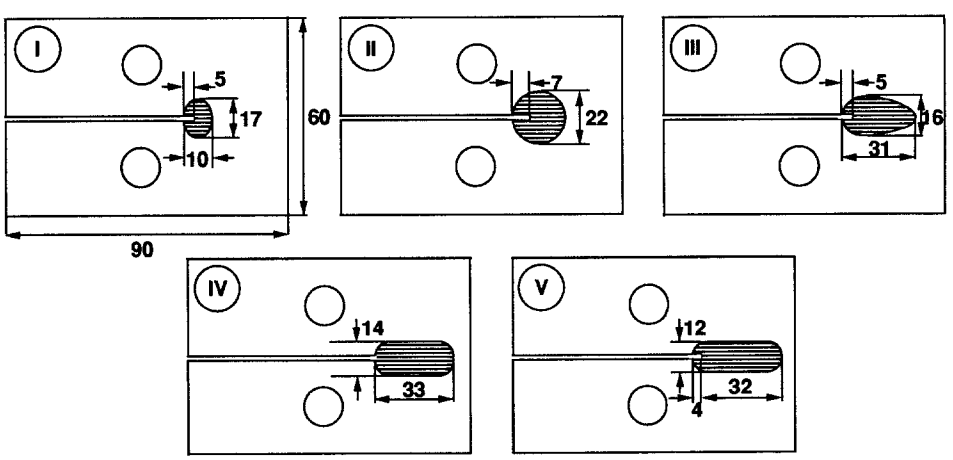

Figure 5 Evolution of the damage zone in different sections of the loading (cf. Figures 2 to 4). Note: the probabilities to find the AE events in the marked damage zones are 97,94,97,99 and 95 % in the sections I to V, respectively [6].

The concluded assignation and ranking of the AE events to the failure observed agree very well with the results published in the literature (e.g.[7]).

4.CONCLUSIONS

The failure mode, caused by monotonic increased loading, was studied in a glass fiber (GF) strand mat reinforced nylon block copolymer (NBC) by simultaneous light microscopic and acoustic emission (AE) monitoring. This technique allowed the reliable assignation of the failure events in the crack tip to the AE events collected. The best correspondance between them was found when the amplitude and energy of the AE signals in selected sections of the loading curve of the compact tension (CT) specimens were regarded.The failure mode was quite different in the crack initiation (up to the load maximum) and crack propagation stages. In the former stage crack tip blunting, whereas in the latter mesh-type deformation of the GF mat with related debonding, fibrillation and fracture of the constituting strands and their filaments took place. The deformation mode of the matrix altered from ductile yielding to viscous tearing when the maximum load was surpassed. The AE analysis in localization mode on enlarged CT-specimens proved to be an adequate tool to assess the damage zone and its development. The size of the damage zone was much larger than observed microscopically. It was shown, that the damage zone reaches its critical size, taken into the loading direction, at the maximum load. In the crack propagation stage this zone flattens and extends along the expected crack growth plane.

ACKNOWLEDGEMENT

The financial support of this study by the EURAM program (MA 1E/0043/C) and that of the research stay of T.Czigány in the Institute for Composite Materials Ltd. in frame of the AIF Project "HT-Thermoplaste" are gratefully acknowledged. Q.Yuan is indebted to the DAAD for the fellowship grant at the University of Kaiserslautern.

REFERENCES

1 J.Karger-Kocsis: Polym.Bull., **24** (1990), 341

2 Idem: ibid., **26** (1991), 123

3 J.Karger-Kocsis: J.Appl.Polym.Sci., (1992) (in press)

4 J.Karger-Kocsis and K.Friedrich: Mechanical properties and failure behavior of glass fiber mat-reinforced nylon RIM composites in "Durability of Polymer Based Composite Systems for Structural Applications" (Eds.:A.H.Cardon and G.Verchery), Elsevier Appl.Sci., Barking, 1991, pp.158-168

5 W.S.Jouri and J.B.Shortall: J.Thermoplast.Compos.Mater.,**4** (1991), 206

6 J.Karger-Kocsis and T.Czigány: J.Mater.Sci. (submitted)

7 H.Hansmann: Materialprüfung, **33** (1991), 304

Accepted April 27, 1992 C